engineering proceedings

MDPI

Proceeding Paper

Sensor Selection and Placement for Track Switch Condition Monitoring through Validated Structural Digital Twin Models of Train–Track Interactions †

Nikhil Pillai [1,*], Jou-Yi Shih [1,2] and Clive Roberts [1]

[1] Birmingham Centre for Railway Research and Education, School of Engineering, University of Birmingham, Birmingham B15 2TT, UK; J.Shih@bham.ac.uk (J.-Y.S.); C.ROBERTS.20@bham.ac.uk (C.R.)
[2] ZynaMic Engineering AB, 120 70 Stockholm, Sweden
* Correspondence: NRP817@bham.ac.uk
† Presented at the 8th International Electronic Conference on Sensors and Applications, 1–15 November 2021; Available online: https://ecsa-8.sciforum.net.

Abstract: Railway track switches experience high failure rates, which can be reduced by monitoring their structural health. The results obtained from a validated Finite Element (FE) model for train–track switch interaction have been introduced to support sensor selection and placement. For the FE models with nominal and damaged rail profiles, virtual strain sensor measurements have been obtained after converting the true strains to engineering strains. Comparisons for the strains before and after the introduction of the fault have demonstrated greater amplitude for the strains after fault introduction. The highest difference in strain amplitude is in the vertical direction, followed by the longitudinal and lateral directions.

Keywords: sensor placement; strain gauges; condition monitoring; switch and crossing (S&C); finite element analysis (FEA); multi-body simulation (MBS)

Citation: Pillai, N.; Shih, J.-Y.; Roberts, C. Sensor Selection and Placement for Track Switch Condition Monitoring through Validated Structural Digital Twin Models of Train–Track Interactions. *Eng. Proc.* **2021**, *10*, 49. https://doi.org/10.3390/ecsa-8-11297

Academic Editor: Francisco Falcone

Published: 1 November 2021

1. Introduction

Switches and Crossings (S&Cs) are components of the track infrastructure that facilitate trains to change track lines. Due to varying cross-sections and the discontinuous rail profiles, S&Cs are subject to a higher failure rate than continuously running rails [1]. The existing approaches for detecting S&C rail failure include visual inspection and condition monitoring. Traditional inspection methods have involved the use of visual judgement and measurement equipment, which are now being complemented with measurement trains fitted with sensors as well as unmanned aerial vehicles.

Continuous condition monitoring of S&Cs is currently carried out to a limited extent and involves the measurement of signals from the Points Operating Equipment (POE) to detect a limited number of failure modes. This has been reviewed by Hamadache et al. [2], where various examples in literature for fault detection and diagnosis for S&Cs were included. Recent research has investigated the installation of sensors on the rails to obtain reliable signals that can be used in fault detection and diagnosis algorithms. In previous research, site measurements were carried out by installing strain gauges and accelerometers at various locations along the length of S&Cs, where a more linear trend was obtained from strain gauges than accelerometers for the measurement of the wheel-rail contact forces for different rolling stock [3]. The appropriate placement of such sensors is of vital importance for successfully detecting faults without redundancy. Numerical simulation approaches have traditionally been used for failure mechanism prediction for S&Cs [4]. They present an efficient alternative to field experimentation for carrying out preliminary studies to support predictive maintenance. Therefore, a novel numerical simulation approach for train S&C track interaction has been implemented to obtain virtual signals from the rail that have been post-processed to determine the orientation and placement of sensors.

2. Methodology

A combined numerical simulation approach based on Multi-Body Simulation (MBS) and Finite Element (FE) analysis was utilised to obtain the outputs necessary to predict the fault locations and determine sensor placement [5]. A holistic MBS model was developed to simulate the dynamic train–track interaction between a Manchester benchmarks passenger vehicle [6] and a 60E1-760-1:14 railway switch [7]. The results from the wheel-rail contact interaction were used to determine the Wear number, Tγ, which has been correlated to the risk of damage occurrence on the rail surface [8]. The detailed 3D FE model shown in Figure 1 was developed for the location with high damage susceptibility. Unlike the MBS model, which is limited to the prediction of forces and stresses at the wheel-rail contact surface, the FE model is able to obtain dynamic response outputs for the subsurface.

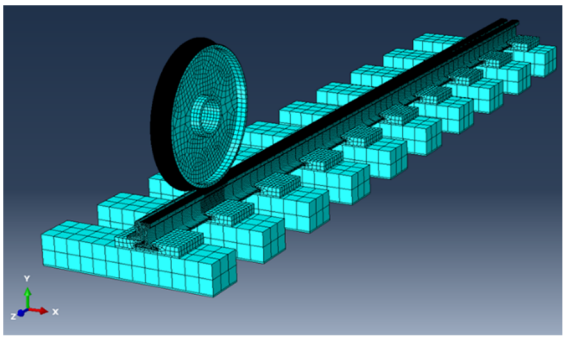

Figure 1. Finite Element model for wheel-switch interaction.

The dynamic behaviour of the track model and the wheel-rail interaction results were validated by comparing the rail receptance and contact force, respectively, against the reference results, as published in [5]. At present, a railhead surface fault has been introduced to this model in the form of a discontinuity on the railhead, as demonstrated in Figure 2a, the geometry of which is influenced by a large "squat" modelled by Bogdański et al. [9]. As shown in Figure 2b, Squats take the form of indentations on the railhead and occur where changes in the track stiffness are observed, such as S&C and rail joints [10,11].

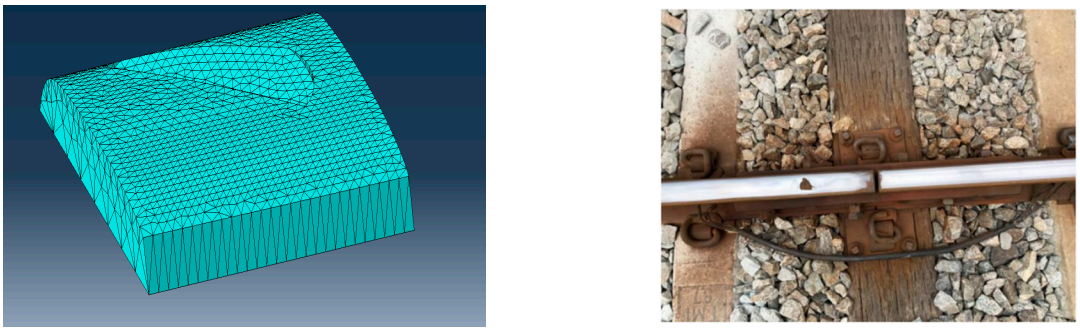

(**a**) (**b**)

Figure 2. (**a**) Modelling the discontinuity on the railhead surface; (**b**) Example of the occurrence of a surface RCF defect in the field [10].

The dynamic train–track interaction simulation has been carried out using FE for the passage of the train at 160 km/hr, both before and after the introduction of the surface fault. Virtual strain sensor measurements were obtained for all rail elements by converting the true strain (ε_t) obtained from FE simulations to the engineering strain (ε_e), which is the actual parameter measured by strain sensors by using the relationship in (1).

$$\varepsilon_t = \ln(1 + \varepsilon_e) \quad (1)$$

The virtual strain measurements before and after introducing the fault were compared and the change in strain due to fault introduction was calculated. The results can help inform the required resolution for the sensors as well as the best locations to install them for fault detection. Similarly, the results for the Von Mises stress, which can help determine the fatigue life of the rail at the potential sensor installation locations have been compared for the models with the nominal and damaged rail profiles.

3. Discussion of Results

The results for the rail strain and stress outputs obtained from the dynamic train–track interaction carried out in FE have been discussed with respect to their utilisation to inform sensor placement.

The surface fault shown in Figure 2 was introduced at a distance of 9.44 m from the beginning of the switch toe. Results have been obtained from the frame at which the wheel passes over the railhead discontinuity and exerts a high impact load on the rail. The results from the same time frame have been obtained for the models with both the nominal and damaged rail profiles. In Figure 3a,b, the Von Mises stress (SMises) on the railhead has been plotted. A higher concentration of stresses on the rail gauge corner at a longitudinal distance of 9.44 to 9.46 m is observed due to the wheel-rail contact patch. Also, higher amplitude of stresses is observed in Figure 3b due to the high impact force resulting from the rail discontinuity. Similarly, in Figure 3c,d, higher amplitude of vertical strains (E22) is observed for the model with the fault. Negative values for the strains denote compression, whilst positive values denote tension. As the wheel, impact force results in high compressive stresses and strains on the railhead; the strain amplitude is mostly negative.

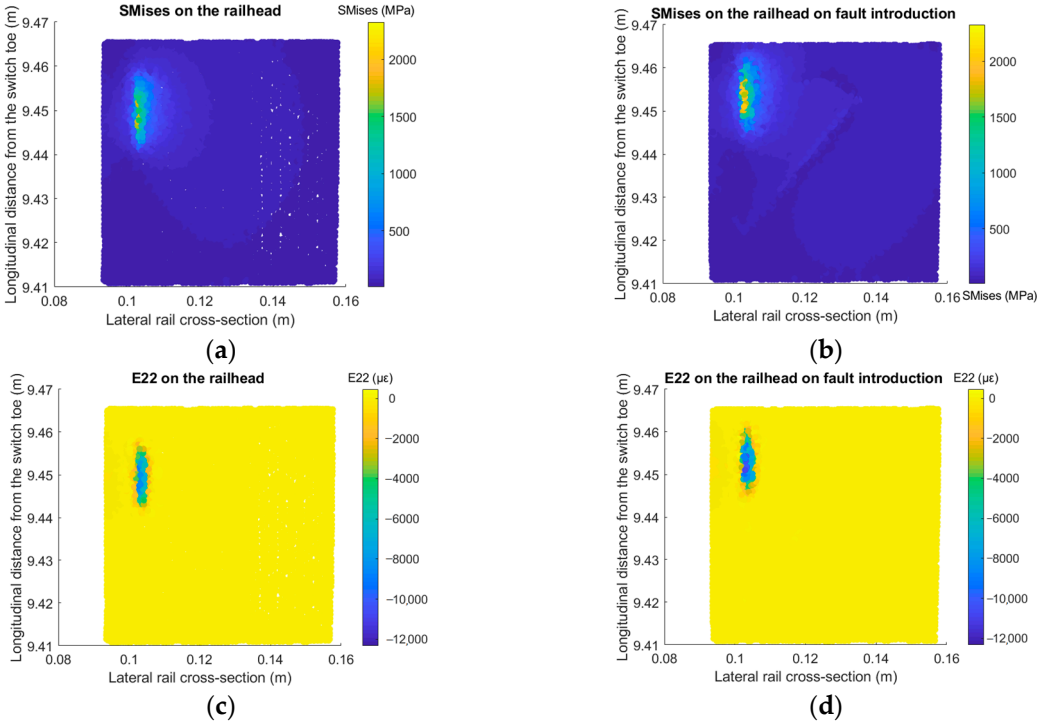

Figure 3. (**a**) Von Mises stress on the railhead-nominal rail; (**b**) Von Mises stress on the railhead-damaged rail; (**c**) Vertical strains on the railhead-nominal rail; (**d**) Vertical strains on the railhead-damaged rail.

As the railhead experiences high stresses and fault initiation, it is more plausible to install sensors away from this region. The results for the strains from the lower portion of the railhead, rail web and foot have been plotted in Figure 4. Strains in the lateral

direction (E11) for the nominal and damaged rail profiles have been plotted in Figure 4a,b, respectively, where high compressive lateral strains are observed at the lower corner of the rail web due to bending. In Figure 4c,d, high compressive strains are observed on the rail web due to the vertical wheel impact load. In Figure 4e,f high compressive longitudinal strains are observed closer to the railhead, whereas tensile strains are observed at the rail foot, demonstrating the expected flexural behaviour. As expected, the strain amplitude is higher for the model with the damage than the nominal rail profile.

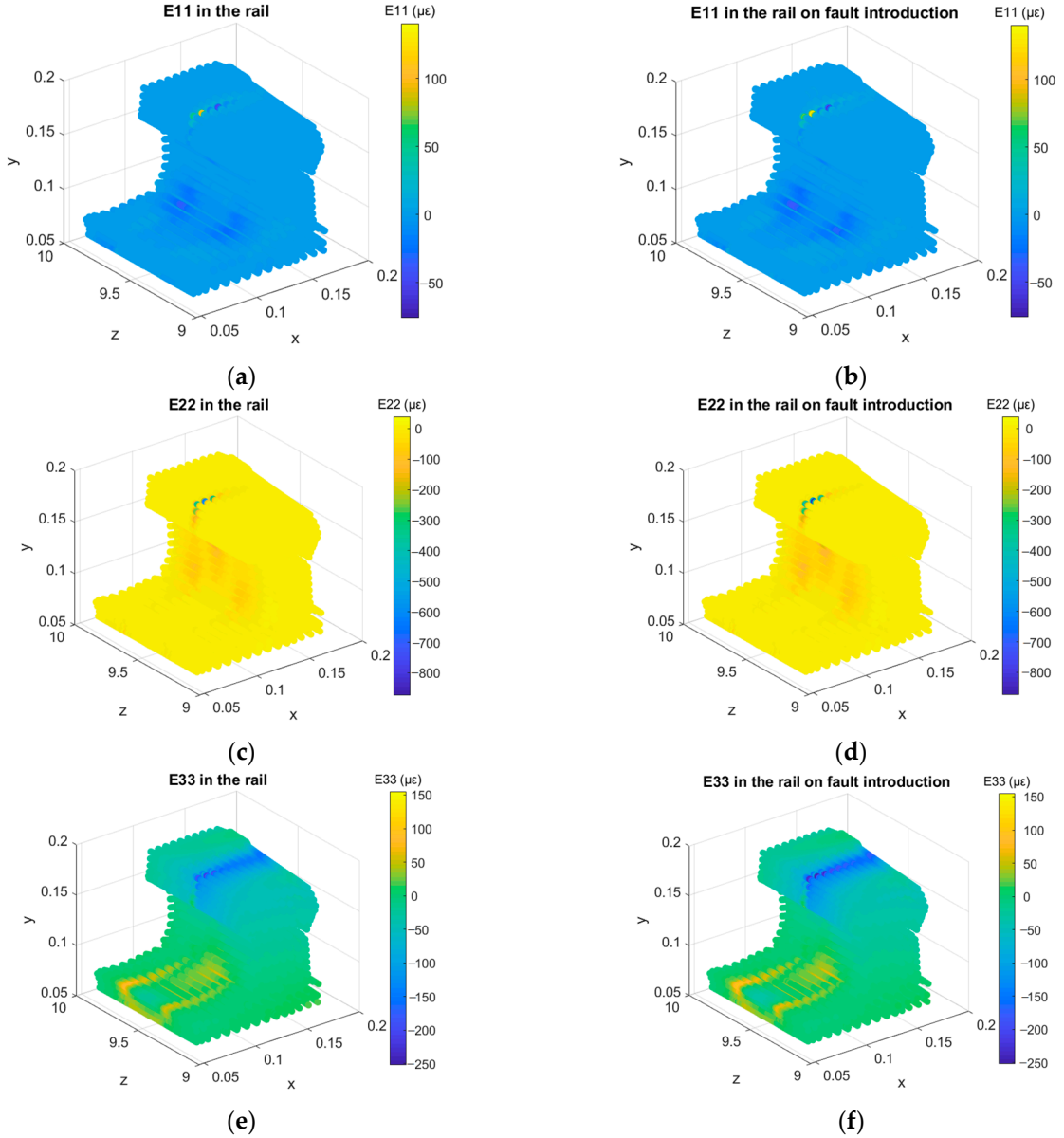

Figure 4. Strains in the rail; (**a**) Lateral strains-nominal rail; (**b**) Lateral strains-damaged rail; (**c**) Vertical strains-nominal rail; (**d**) Vertical strains-damaged rail; (**e**) Longitudinal strains-nominal rail; (**f**) Longitudinal strains-damaged rail.

The strain amplitude in the rail web and foot in Figure 4 are large enough to be detected using strain sensors. However, the detection of fault would require the determination of adequate sensor resolution to measure the change in strain resulting from the fault occurrence. Therefore, the change in strain amplitude due to fault introduction have been plotted in Figure 5. The highest change in strain is observed in the vertical direction since it is also the amplitude of strains in the vertical direction that is the highest. The second

highest change is observed for the longitudinal strains followed by the lateral strains. Hence, the placement of sensors on the YZ plane or the sides of the rail would help sense a higher difference in strain amplitudes on fault occurrence. The placement of sensors in the XZ plane or the rail bottom will also help capture an adequate difference in strains, with improved fatigue life of the sensor.

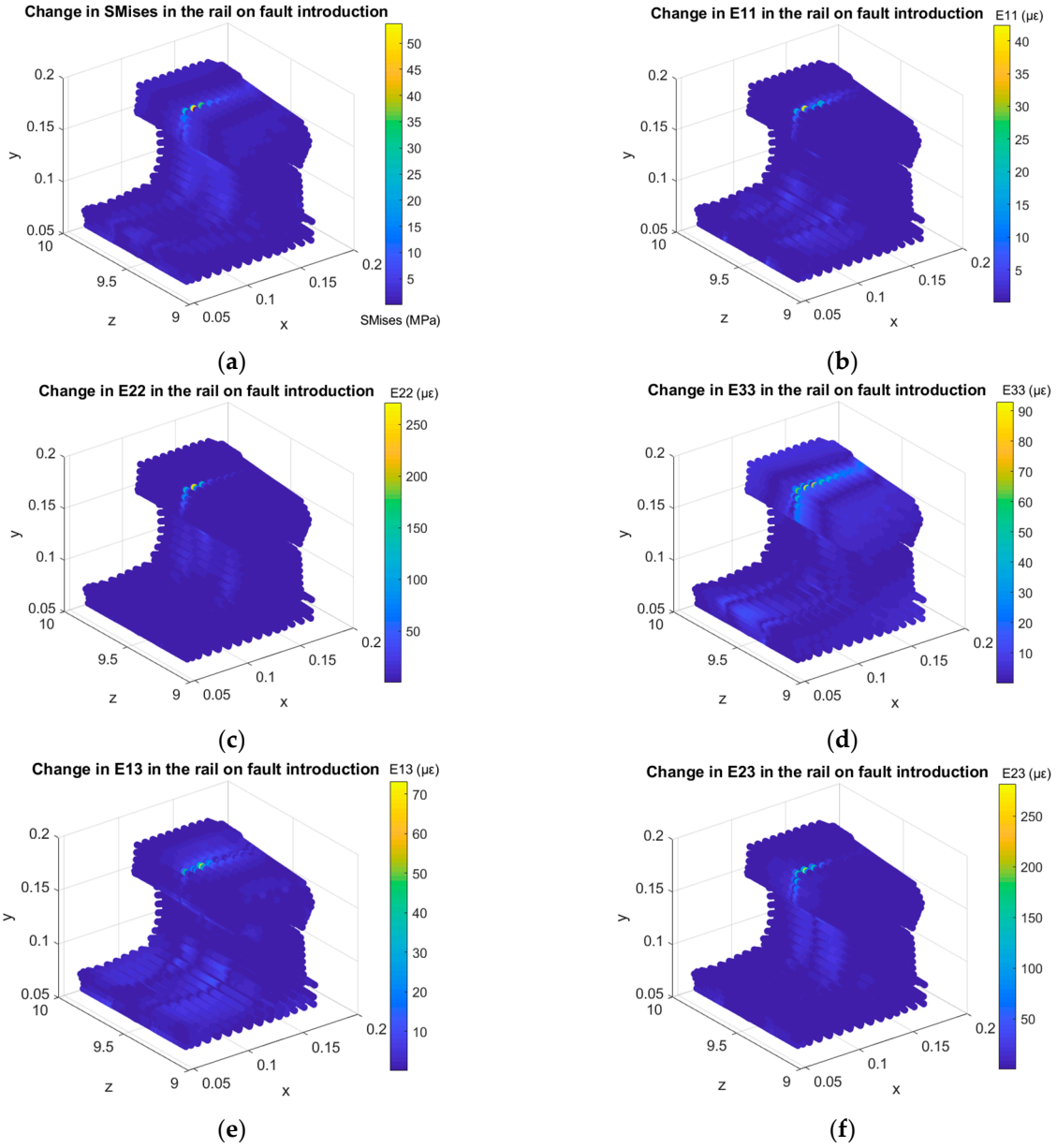

Figure 5. Difference in results on fault introduction; (**a**) Difference in Von Mises stress; (**b**) Difference in horizontal/lateral strain (E11); (**c**) Difference in vertical/normal strain (E22); (**d**) Difference in longitudinal strain (E33); (**e**) Difference in shear stress in the X-Z plane; (**f**) Difference in shear stress in the X-Y plane.

4. Conclusions and Future Work

Validated simulations of train–track switch interactions have been used to inform strain sensor placement for predictive maintenance. The FE simulations were carried out for a switch model with nominal rail profiles and after introducing surface damage. Higher strain and stress outputs have been obtained after introducing surface rail damage. The overall amplitude for the rail strains as well as its change on fault introduction is the

highest in the vertical direction, followed by the longitudinal and lateral directions. Further analysis of the modelling results will be carried out to determine detailed positioning of sensors based on the rail fatigue life, risk of fault occurrence and measurement redundancy. Similarly, parametric simulation studies for different railway traffic conditions will be input to inform sensor placement. As the present work is limited to modelling a specific surface defect, future work will involve introducing worn rail profiles and change in track stiffness into the model for determining sensor placement to detect multiple faults. Additional complexities can be introduced into the models and a bigger dataset can be statistically analysed for determining sensor placement. With the availability of data for live traffic, Digital Twin models of different routes could enable intelligent decisions for supporting condition monitoring and risk-informed predictive maintenance.

Author Contributions: Conceptualization, N.P.; methodology, N.P.; data curation, N.P.; writing—original draft preparation, N.P.; writing—review and editing, N.P. and J.-Y.S.; visualization, N.P.; supervision, J.-Y.S. and C.R.; funding acquisition, C.R. All authors have read and agreed to the published version of the manuscript.

Funding: The work described has been supported by the S-CODE project. This project has received funding from the Shift2Rail Joint Undertaking under the European Union's Horizon 2020 research and innovation programme under grant agreement No. 730849. This publication reflects only the authors' view, and the Shift2Rail Joint Undertaking is not responsible for any use that may be made of the information it contains.

Institutional Review Board Statement: Not applicable.

Informed Consent Statement: Not applicable.

Data Availability Statement: The data presented in this study are available on request from the corresponding author. Other studies from the ongoing research have been published in [4,5].

Conflicts of Interest: The authors declare no conflict of interest.

References

1. Cornish, A.; Smith, R.A.; Dear, J. Monitoring of strain of in-service railway switch rails through field experimentation. *Proc. Inst. Mech. Eng. Part F J. Rail Rapid Transit* **2016**, *230*, 1429–1439. [CrossRef]
2. Hamadache, M.; Dutta, S.; Olaby, O.; Ambur, R.; Stewart, E.; Dixon, R. On the fault detection and diagnosis of railway switch and crossing systems: An overview. *Appl. Sci.* **2019**, *9*, 5129. [CrossRef]
3. Shih, J.-Y.; Weston, P.; Pillai, N.; Entezami, M.; Stewart, E.; Roberts, C. Potential condition monitoring system for switch and crossings using accelerometers. In Proceedings of the 13th International Workshop on Railway Noise, Ghent, Belgium, 16–20 September 2019; pp. 2019–2020.
4. Pillai, N.; Shih, J.Y.; Roberts, C. Evaluation of numerical simulation approaches for simulating train-track interactions and predicting rail damage in railway switches and crossings (S&Cs). *Infrastructures* **2021**, *6*, 63. [CrossRef]
5. Pillai, N.; Shih, J.Y.; Roberts, C. Enabling data-driven predictive maintenance for Switch and Crossing (S&C) through Digital Twin models and condition monitoring systems. *J. Perm. Way Inst.* **2021**, *139*, 14–20.
6. Iwnicki, S. Manchester benchmarks for rail vehicle simulation. *Veh. Syst. Dyn.* **1998**, *30*, 295–313. [CrossRef]
7. Bezin, Y.; Pålsson, B.A. Multibody simulation benchmark for dynamic vehicle-track interaction in switches and crossings: Modelling description and simulation tasks. *Veh. Syst. Dyn.* **2021**, 1–16. [CrossRef]
8. Burstow, M. Whole Life Rail Model Application and Development: Development of a Rolling Contact Fatigue Damage Parameter (Burstow Report). 2003. Available online: https://www.sparkrail.org/Lists/Records/DispForm.aspx?ID=9396 (accessed on 1 February 2021).
9. Bogdański, S.; Olzak, M.; Stupnicki, J. Numerical modelling of a 3D rail RCF 'squat'-type crack under operating load. *Fatigue Fract. Eng. Mater. Struct.* **1998**, *21*, 923–935. [CrossRef]
10. Cho, H.; Park, J. Study of rail squat characteristics through analysis of train axle box acceleration frequency. *Appl. Sci.* **2021**, *11*, 7022. [CrossRef]
11. Li, Z.; Zhao, X.; Dollevoet, R.; Molodova, M. Differential wear and plastic deformation as causes of squat at track local stiffness change combined with other track short defects. *Veh. Syst. Dyn.* **2008**, *46*, 237–246. [CrossRef]